Angewandte Chemie
Eine Zeitschrift der Gesellschaft Deutscher Chemiker

Supporting Information

Oxygen Activation at the Active Site of a Fungal Lytic Polysaccharide Monooxygenase

*William B. O'Dell, Pratul K. Agarwal, and Flora Meilleur**

anie_201610502_sm_miscellaneous_information.pdf

Table of Contents:

Abbreviated main text citations given in full

[1a] P. V. Harris, D. Welner, K. C. McFarland, E. Re, J. C. N. Poulsen, K. Brown, R. Salbo, H. S. Ding, E. Vlasenko, S. Merino, F. Xu, J. Cherry, S. Larsen, L. Lo Leggio, *Biochemistry* **2010**, *49*, 3305-3316.

[4] C. H. Kjaergaard, M. F. Qayyum, S. D. Wong, F. Xu, G. R. Hemsworth, D. J. Walton, N. A. Young, G. J. Davies, P. H. Walton, K. S. Johansen, K. O. Hodgson, B. Hedman, E. I. Solomon, *Proc. Natl. Acad. Sci. U. S. A.* **2014**, *111*, 8797-8802.

[8] M. Gudmundsson, S. Kim, M. Wu, T. Ishida, M. H. Momeni, G. Vaaje-Kolstad, D. Lundberg, A. Royant, J. Stahlberg, V. G. H. Eijsink, G. T. Beckham, M. Sandgren, *J. Biol. Chem.* **2014**, *289*, 18782-18792.

[11] K. E. Frandsen, T. J. Simmons, P. Dupree, J. C. Poulsen, G. R. Hemsworth, L. Ciano, E. M. Johnston, M. Tovborg, K. S. Johansen, P. von Freiesleben, L. Marmuse, S. Fort, S. Cottaz, H. Driguez, B. Henrissat, N. Lenfant, F. Tuna, A. Baldansuren, G. J. Davies, L. Lo Leggio, P. H. Walton, *Nature Chem. Biol.* **2016**, *12*, 298-303.

[12a] N. Colloc'h, L. Gabison, G. Monard, M. Altarsha, M. Chiadmi, G. Marassio, J. S. D. O. Santos, M. El Hajji, B. Castro, J. H. Abraini, T. Prange, *Biophys. J.* **2008**, *95*, 2415-2422.

Experimental details

Crystallization and crystal soaking

Heterologous protein production of *Nc*PMO-2 from *Pichia pastoris* host, crystallization and data collection methods used are described elsewhere by O'Dell *et al.* Protein was crystallized for these studies as expressed with respect to the bound metal ion. X-ray fluorescence scans of crystals from "as expressed" protein, Figure S7, showed an edge centered at 8984 electron volts (eV) corresponding to copper(I) which can be attributed to the facile photoreduction of the copper ion in X-ray fluorescence studies.[S1] (Scans near absorption edges of other metals were not performed.) The crystallization behaviors of metal-exchanged forms of *Nc*PMO-2 were used to confirm further that the active site of the crystallized protein predominantly contains a copper ion as opposed to nickel or zinc which have been observed in other AA9 LPMO structures.[S2, 3] Apo-*Nc*PMO-2 was prepared by treating the protein with agarose-immobilized nitrilotriacetic acid.[S4, 5] Reconstituting the metal coordination site by diluting apo-*Nc*PMO-2 to a 100-fold molar excess of 10 mM $CuCl_2$ in 20 mM $Na(CH_3COO^-)$, incubation for two hours, concentration and chromatographic desalting resulted in Cu holo-*Nc*PMO-2 with identical crystallization behavior of the "as expressed" protein. Reconstituting apo-*Nc*PMO-2 with either 10 mM $NiSO_4$ or 10 mM $ZnCl_2$ yielded holo-*Nc*PMO-2 which would not crystallize under the precipitant and pH conditions used to crystallize "as expressed" *Nc*PMO-2 for this study.

For ascorbate-treated structures, crystals were harvested and transferred to a soaking solution containing 100 mM HEPES, 100 mM ascorbic acid pH = 6.0 and 25%

(wt./vol.) PEG 3350. Crystals were incubated at room temperature for two hours prior to flash freezing for data collection. All crystal manipulations were conducted in air.

Model refinement

X-ray diffraction intensities and starting atomic coordinates derived from PDB 4EIR were used for molecular replacement with *Phaser* as implemented in *PHENIX*.[S6-8] Automated structure rebuilding of the resulting model by *PHENIX AutoBuild* was used to minimize phase bias from the replacement model.[S9] Models were refined against X-ray data using *phenix.refine*.[S10] For PDB 5TKI neutron data were added to the model after several rounds of refinement against the X-ray data so that the model was jointly refined against X-ray data for heavy atoms and neutron data for hydrogen and deuterium atoms.[S11] The conformation and protonation state of His157 was determined by refining single N_δ protonated, single N_ε protonated and double N_δ,N_ε protonated forms against the neutron scattering length density in the two sidechain conformations that could be fitted to the electron density. (Here, "protonated" refers to 100% occupancy of ^{2}H due to the ^{1}H/^{2}H exchange of the protein crystal prior to neutron and X-ray diffraction measurement.)

Dataset and final refinement statistics shown for all models in Tables S1 and S2 were calculated using *phenix.table_one*.[S12] The precision of atomic coordinates in the models 5TKG (0.030 Å average) and 5TKH (0.035 Å average) were estimated by evaluating the Cruickshank diffraction precision index for the model as implemented in the web server *Online_DPI*.[S13-15] Selected coordinate precision estimates are reported in Tables S3 and S4. Simple omit maps for the dioxygen species observed in

5TKG and 5TKH were calculated by removing the oxygen atom proximal to copper, distal to copper or both oxygen atoms and calculating F_O–F_C difference electron density. Positive contours of the F_O–F_C density extending for 10.0 Å around the omitted atoms are shown in Fig. S1.

Multiple sequence alignment

Amino acid sequences of the crystallized portions of AA9 LPMOs *Neurospora crassa* PMO-2, *Neurospora crassa* PMO-3, *Neurospora crassa* LPMO9-F, *Neurospora crassa* LPMO9-C, *Lentinus similis* (AA9)-A, *Phanerochaete chrysosporium* GH61-D, *Thermoascus aurantiacus* GH61-A, *Thelavia terrestris* GH61-E and *Trichoderma reesei* CEL61B were obtained from PDB entries 5TKG, 4EIS, 4QI8, 4D7U, 5ACF, 4B5Q, 2YET, 3EII, and 2VTC, respectively. Multiple sequence alignment was performed with the T-coffee server, and results were formatted using ESPript.[S16, 17]

Density functional theory calculations

The three active site models (ASMs) used for DFT calculation were derived by extracting coordinates from the resting state X-ray structure (PDB 5TKG) including residues His1, His84, His157, Gln166 and Tyr168 along with the active site copper(II) ion, pre-bound molecular O_2 and the axial and equatorial water molecules as shown in Fig S3. To reduce the total number of atoms in the ASMs, residues His84, His157, Gln166 and Tyr168 were truncated at C_β which was modeled as a methyl group. DFT calculations were performed with Gaussian 09 using the uB3LYP functional with the 6-31g** basis set applied to all atoms.[S18] The model was implicitly solvated using the

polarizable continuum model as implemented in Gaussian 09 with a dielectric constant of 4.24. For geometry optimization, the coordinates of one heavy atom per residue, indicated by a star in Figure S3, were constrained to their starting values to maintain the relative conformation imposed by the protein backbone. Molecular O_2 "pre-binding" energies were estimated by the difference between two forms of each ASM: one with molecular O_2 occupying the pre-binding site and the other with molecular O_2 moved to a distance >10 Å from other atoms in the model and the pre-binding site left vacant.

References

S1. Kjaergaard, C.H., M.F. Qayyum, S.D. Wong, F. Xu, G.R. Hemsworth, D.J. Walton, N.A. Young, G.J. Davies, P.H. Walton, K.S. Johansen, K.O. Hodgson, B. Hedman, and E.I. Solomon, *Spectroscopic and computational insight into the activation of O_2 by the mononuclear Cu center in polysaccharide monooxygenases.* Proceedings of the National Academy of Sciences of the United States of America, 2014. **111**(24): p. 8797-8802.

S2. Karkehabadi, S., H. Hansson, S. Kim, K. Piens, C. Mitchinson, and M. Sandgren, *The First Structure of a Glycoside Hydrolase Family 61 Member, Cel61B from Hypocrea jecorina, at 1.6 angstrom Resolution.* Journal of Molecular Biology, 2008. **383**(1): p. 144-154.

S3. Harris, P.V., D. Welner, K.C. McFarland, E. Re, J.C.N. Poulsen, K. Brown, R. Salbo, H.S. Ding, E. Vlasenko, S. Merino, F. Xu, J. Cherry, S. Larsen, and L. Lo Leggio, *Stimulation of Lignocellulosic Biomass Hydrolysis by Proteins of Glycoside Hydrolase Family 61: Structure and Function of a Large, Enigmatic Family.* Biochemistry, 2010. **49**(15): p. 3305-3316.

S4. Carrer, C., M. Stolz, E. Lewitzki, C. Rittmeyer, B.O. Kolbesen, and E. Grell, *Removing coordinated metal ions from proteins: a fast and mild method in aqueous solution.* Analytical and Bioanalytical Chemistry, 2006. **385**(8): p. 1409-1413.

S5. Quinlan, R.J., M.D. Sweeney, L. Lo Leggio, H. Otten, J.C.N. Poulsen, K.S. Johansen, K. Krogh, C.I. Jorgensen, M. Tovborg, A. Anthonsen, T. Tryfona, C.P. Walter, P. Dupree, F. Xu, G.J. Davies, and P.H. Walton, *Insights into the oxidative degradation of cellulose by a copper metalloenzyme that exploits biomass components.* Proceedings of the National Academy of Sciences of the United States of America, 2011. **108**(37): p. 15079-15084.

S6. Mccoy, A.J., R.W. Grosse-Kunstleve, P.D. Adams, M.D. Winn, L.C. Storoni, and R.J. Read, *Phaser crystallographic software.* Journal of Applied Crystallography, 2007. **40**: p. 658-674.

S7. Adams, P.D., P.V. Afonine, G. Bunkoczi, V.B. Chen, I.W. Davis, N. Echols, J.J. Headd, L.W. Hung, G.J. Kapral, R.W. Grosse-Kunstleve, A.J. McCoy, N.W. Moriarty, R. Oeffner, R.J. Read, D.C. Richardson, J.S. Richardson, T.C. Terwilliger, and P.H. Zwart, *PHENIX: a comprehensive Python-based system for macromolecular structure solution.* Acta Crystallographica, Section D: Biological Crystallography, 2010. **66**(Pt 2): p. 213-21.

S8. Li, X., W.T. Beeson, C.M. Phillips, M.A. Marletta, and J.H.D. Cate, *Structural Basis for Substrate Targeting and Catalysis by Fungal Polysaccharide Monooxygenases.* Structure, 2012. **20**(6): p. 1051-1061.

S9. Terwilliger, T.C., R.W. Grosse-Kunstleve, P.V. Afonine, N.W. Moriarty, P.H. Zwart, L.W. Hung, R.J. Read, and P.D. Adams, *Iterative model building, structure refinement and density modification with the PHENIX AutoBuild wizard.* Acta Crystallographica Section D-Biological Crystallography, 2008. **64**: p. 61-69.

S10. Afonine, P.V., R.W. Grosse-Kunstleve, N. Echols, J.J. Headd, N.W. Moriarty, M. Mustyakimov, T.C. Terwilliger, A. Urzhumtsev, P.H. Zwart, and P.D. Adams, *Towards automated crystallographic structure refinement with phenix.refine.* Acta Crystallographica, Section D: Biological Crystallography, 2012. **68**(Pt 4): p. 352-67.

S11. Afonine, P.V., M. Mustyakimov, R.W. Grosse-Kunstleve, N.W. Moriarty, P. Langan, and P.D. Adams, *Joint X-ray and neutron refinement with phenix.refine.* Acta Crystallographica, Section D: Biological Crystallography, 2010. **66**(Pt 11): p. 1153-63.

S12. Afonine, P.V., R.W. Grosse-Kunstleve, V.B. Chen, J.J. Headd, N.W. Moriarty, J.S. Richardson, D.C. Richardson, A. Urzhumtsev, P.H. Zwart, and P.D. Adams, *phenix.model_vs_data: a high-level tool for the calculation of crystallographic model and data statistics.* J Appl Crystallogr, 2010. **43**(Pt 4): p. 669-676.

S13. Cruickshank, D., *Remarks about protein structure precision.* Acta Crystallographica Section D, 1999. **55**(3): p. 583-601.

S14. Gurusaran, M., M. Shankar, R. Nagarajan, J.R. Helliwell, and K. Sekar, *Do we see what we should see? Describing non-covalent interactions in protein structures including precision.* IUCrJ, 2014. **1**(1): p. 74-81.

S15. Kumar, K.S.D., M. Gurusaran, S.N. Satheesh, P. Radha, S. Pavithra, K.P.S. Thulaa Tharshan, J.R. Helliwell, and K. Sekar, *Online_DPI: a web server to calculate the diffraction precision index for a protein structure.* Journal of Applied Crystallography, 2015. **48**(3): p. 939-942.

S16. Robert, X. and P. Gouet, *Deciphering key features in protein structures with the new ENDscript server.* Nucleic Acids Research, 2014. **42**(W1): p. W320-W324.

S17. Di Tommaso, P., S. Moretti, I. Xenarios, M. Orobitg, A. Montanyola, J.-M. Chang, J.-F. Taly, and C. Notredame, *T-Coffee: a web server for the multiple sequence alignment of protein and RNA sequences using structural information and homology extension.* Nucleic Acids Research, 2011. **39**(suppl 2): p. W13-W17.

S18. Frisch, M.J., G.W. Trucks, H.B. Schlegel, G.E. Scuseria, M.A. Robb, J.R. Cheeseman, G. Scalmani, V. Barone, B. Mennucci, G.A. Petersson, H. Nakatsuji, M. Caricato, X. Li, H.P. Hratchian, A.F. Izmaylov, J. Bloino, G. Zheng, J.L. Sonnenberg, M. Hada, M. Ehara, K. Toyota, R. Fukuda, J. Hasegawa, M. Ishida, T. Nakajima, Y. Honda, O. Kitao, H. Nakai, T. Vreven, J.A. Montgomery

Jr., J.E. Peralta, F. Ogliaro, M.J. Bearpark, J. Heyd, E.N. Brothers, K.N. Kudin, V.N. Staroverov, R. Kobayashi, J. Normand, K. Raghavachari, A.P. Rendell, J.C. Burant, S.S. Iyengar, J. Tomasi, M. Cossi, N. Rega, N.J. Millam, M. Klene, J.E. Knox, J.B. Cross, V. Bakken, C. Adamo, J. Jaramillo, R. Gomperts, R.E. Stratmann, O. Yazyev, A.J. Austin, R. Cammi, C. Pomelli, J.W. Ochterski, R.L. Martin, K. Morokuma, V.G. Zakrzewski, G.A. Voth, P. Salvador, J.J. Dannenberg, S. Dapprich, A.D. Daniels, Ö. Farkas, J.B. Foresman, J.V. Ortiz, J. Cioslowski, and D.J. Fox, *Gaussian 09*, 2009, Gaussian, Inc.: Wallingford, CT, USA.

Table S1. X-ray and neutron crystallographic data statistics.

PDB ID	**5TKG**	**5TKH**	**5TKI**	**5TKI**
Incident Radiation	X-ray	X-ray	X-ray	Neutron
Wavelength (Å)	1.00	1.00	1.54	2.85-4.50
Resolution range (Å)	28.73 – 1.20 (1.24 – 1.20)	31.82 – 1.20 (1.243 – 1.20)	36.10 – 1.50 (1.55 – 1.50)	32.87 – 2.12 (2.19 – 2.12)
Space group	P 1 21 1	P 1 21 1	P 1 21 1	P 1 21 1
Unit cell (*a*, *b*, *c*) (Å)	67.35, 42.21, 69.48	67.17, 42.24, 69.37	68.12, 42.23, 70.29	68.12, 42.23, 70.29
(*α*, *β*, *γ*) (°)	90, 98.96, 90	90, 98.65, 90	90, 98.33, 90	90, 98.33, 90
Total reflections	228097 (21939)	227779 (22042)	224095 (20772)	31698 (2251)
Unique reflections	117125 (11360)	115269 (11178)	58482 (5409)	18141 (1381)
Multiplicity	1.9 (1.9)	2.0 (2.0)	3.8 (3.8)	1.7 (1.6)
Completeness (%)	97.0 (94.6)	95.7 (93.4)	90.2 (80.3)	79.0 (61.0)
Mean intensity/sigma(intensity)	7.21 (4.18)	5.86 (4.23)	13.8 (4.2)	4.9 (3.6)
Wilson B-factor (Å^2)	8.77	8.37	16.04	8.08
R_{merge}	0.0732 (0.1512)	0.1091 (0.1416)	0.0540 (0.3406)	0.1277 (0.1903)
R_{meas}	0.1034 (0.2138)	0.1543 (0.2003)	0.0633 (0.3963)	0.1806 (0.2691)
CC1/2	0.982 (0.897)	0.950 (0.895)	0.999 (0.892)	0.926 (0.754)

Table S2. X-ray and neutron model refinement statistics.

PDB ID	5TKG	5TKH	5TKI (X-ray)	5TKI (neutron)
Reflections used in refinement	117101 (11354)	115249 (11177)	57483 (5061)	18134 (1381)
Reflections used for R-free	1997 (202)	1992 (203)	1967 (174)	630 (54)
R-work	0.1142 (0.1275)	0.1279 (0.1174)	0.1476 (0.2550)	0.2142 (0.3143)
R-free	0.1399 (0.1650)	0.1540 (0.1619)	0.1790 (0.2901)	0.2508 (0.3562)
CC(work)	0.977 (0.964)	0.953 (0.956)	0.980 (0.893)	0.886 (0.485)
CC(free)	0.968 (0.926)	0.912 (0.960)	0.980 (0.837)	0.830 (0.105)
Number of non-hydrogen atoms	4699	4503	3841	3841
Macromolecules	3705	3578	3404	3404
Ligands	73	62	58	58
Solvent	921	863	379	379
Protein residues	446	446	446	446
RMS(bonds)	0.009	0.008	0.015	0.015
RMS(angles)	1.18	1.10	1.45	1.45
Ramachandran favored (%)	97.0	96.0	96.0	96.0
Ramachandran allowed (%)	2.9	2.9	2.7	2.7
Ramachandran outliers (%)	0.23	0.68	0.9	0.9
Rotamer outliers (%)	1.7	1.3	2.4	2.4
Clash score	2.01	1.67	4.40	9.99
Average B-factor	14.44	13.66	21.54	21.54
Macromolecules	11.30	10.89	20.04	20.04
Ligands	23.56	22.02	36.09	36.09
Solvent	26.34	24.53	32.75	32.75

Table S3. Copper–ligand distances and selected atomic displacement factors in the resting state active site structure (PDB 5TKG).

	Molecule A	Molecule B
Atomic displacement factor (Å^2)[a]		
copper(II) ion	8.40	7.44
equatorial water	13.68	12.25
axial water	17.33	16.06
pre-bound oxygen	19.68	18.85
Occupancies		
copper(II) ion	1.00	1.00
equatorial water	1.00	1.00
axial water	1.00	1.00
pre-bound oxygen	0.49	0.57
Coordinate error (DPI estimate)[b] (Å)		
copper(II) ion	0.023	0.021
equatorial water	0.029	0.027
axial water	0.032	0.031
pre-bound oxygen (O1, O2)	0.035, 0.035	0.034, 0.034
Distances (Å)		
Cu–H1-N_δ	1.96	1.96
Cu–H1-N_{amino}	2.13	2.09
Cu–H84-N_ε	2.00	1.99
Cu–Y168-OH	2.64	2.59
Cu–$H_2O_{equatorial}$	2.00	1.96
Cu–H_2O_{axial}	2.44	2.36
Cu–O1	4.61	4.91
O1–O2	1.21	1.20

a. All non-hydrogen atoms in the model were refined with anisotropic atomic displacement parameters. Converted isotropic *B*-factors are shown here.
b. diffraction precision index

Table S4. Copper–ligand distances and selected atomic displacement factors in the ascorbate-treated active site structure (PDB 5TKH).

	Molecule A	Molecule B
Atomic displacement factor (Å^2)[a]		
copper(II) ion	8.39	9.07
equatorial water	--	34.60
axial water	28.14	29.21
peroxide	18.98	--
pre-bound oxygen	--	26.27
Occupancies (%)		
copper(II) ion	1.00	1.00
equatorial water	--	0.60
axial water	0.48	0.34
peroxide	0.59	--
pre-bound oxygen	--	0.60
Coordinate error (DPI estimate)[b] (Å)		
copper(II) ion	0.027	0.028
equatorial water	--	0.055
axial water	0.050	0.051
peroxide (O1, O2)	0.041, 0.041	--
pre-bound oxygen (O1, O2)	--	0.048, 0.048
Distances (Å)		
Cu–H1-N_{δ}	1.93	1.95
Cu–H1-N_{amino}	2.19	2.20
Cu–H84-N_{ε}	1.97	1.90
Cu–Y168-OH	2.66	2.73
Cu–$H_2O_{equatorial}$	--	2.06
Cu–H_2O_{axial}	2.36	2.23
Cu–O1	1.90	3.57
O1–O2	1.44	1.20

a. All non-hydrogen atoms in the model were refined with anisotropic atomic displacement parameters. Converted isotropic *B*-factors are shown here.
b. diffraction precision index

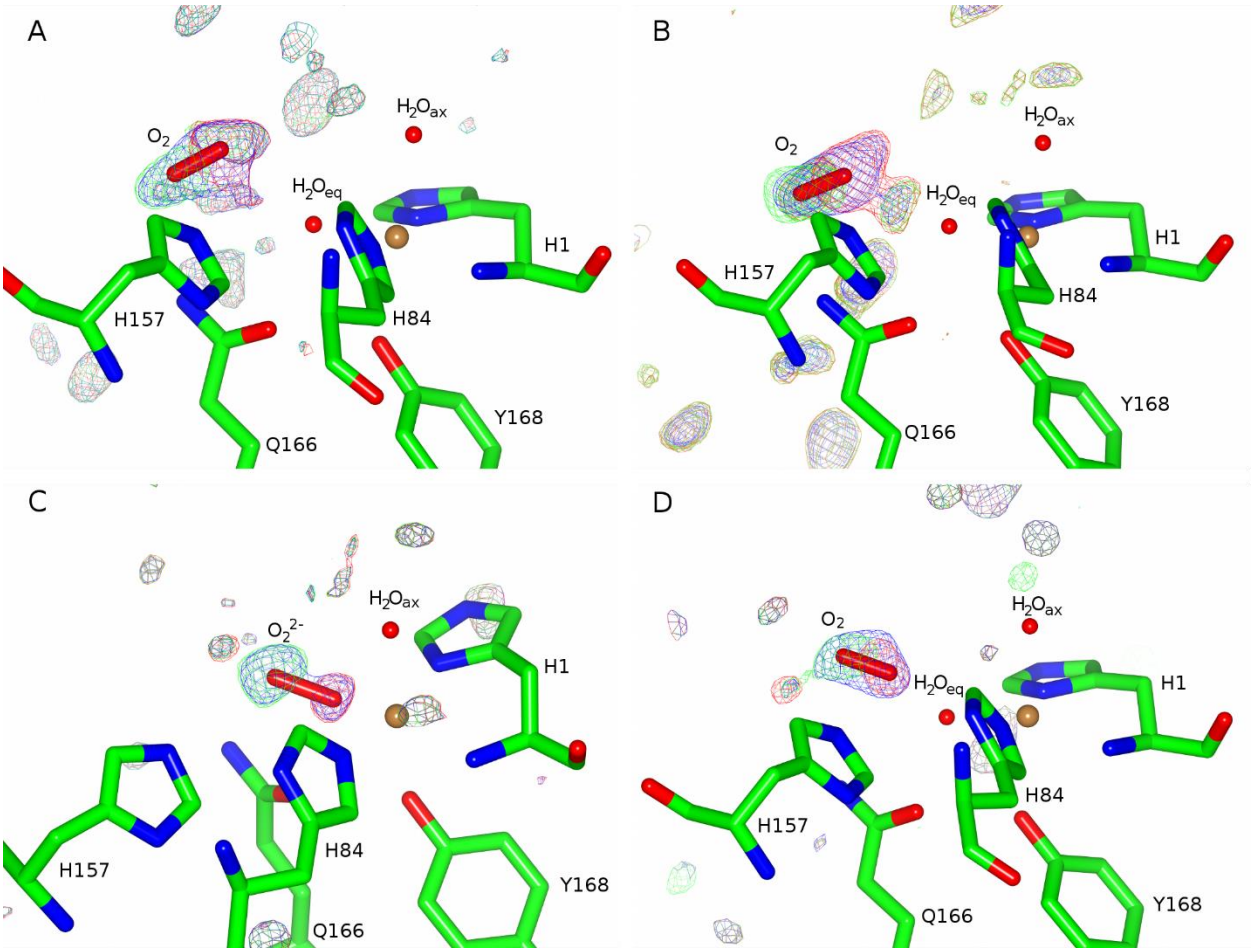

Figure S1. Electron density F_O–F_C omit maps for oxygen species in untreated and ascorbate-treated X-ray models. Panels A-B show NCS molecules A and B of 5TKG (resting state) with omit density calculated for molecular oxygen. Panels C-D show NCS molecules A and B of 5TKH (ascorbate treated) with omit density calculated for peroxide and molecular oxygen. Omit maps are contoured at σ = 3.5 with density (positive F_O–F_C contours) from omitting both oxygens, the proximal oxygen and the distal oxygen shown in blue, red and green, respectively. Maps extend 10.0 Å radially around the omitted oxygen atoms.

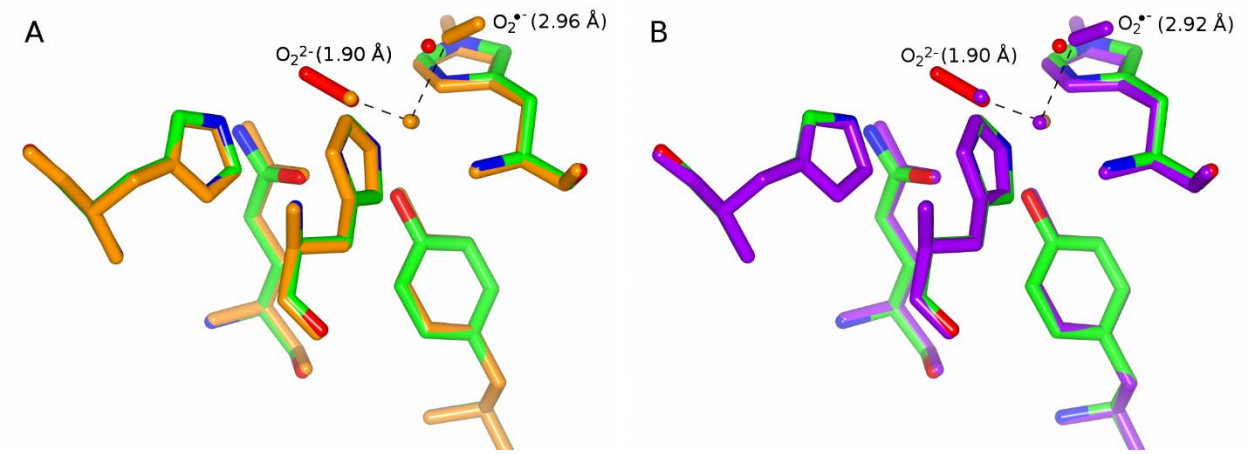

Figure S2. Superposition of copper–dioxo model (PDB 5TKH) with PDB 4EIR. Panel A shows PDB 5TKH NCS molecule A superimposed with PDB 4EIR NCS molecule A (orange) along with the identity of the oxygen species in the respective models and the Cu–O1 distance. Panel B shows the same comparison for PDB 4EIR NCS molecule B (purple).

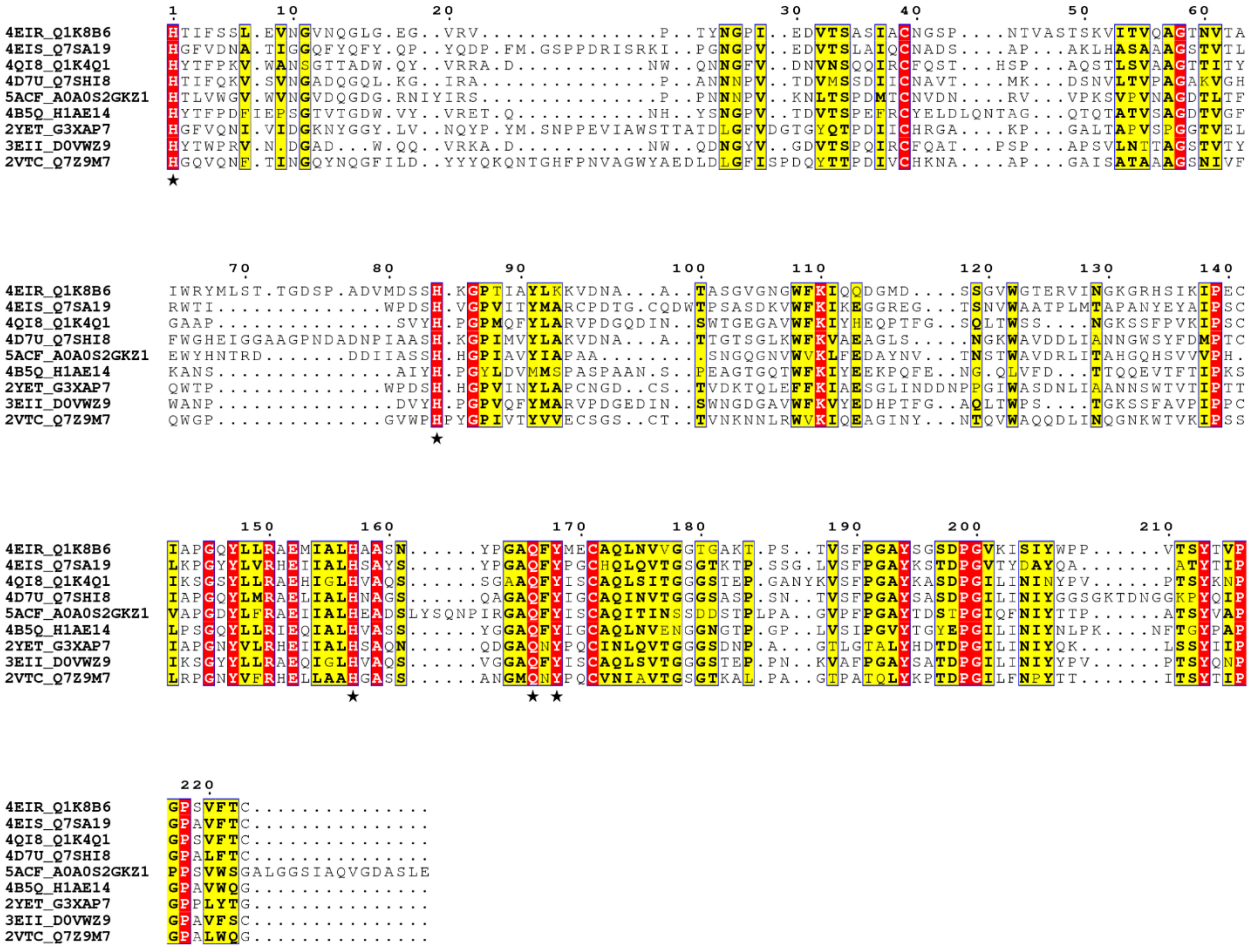

Figure S3. Multiple sequence alignment of AA9 proteins with known crystal structures. Sequences are identified by PDB and Uniprot accession codes. Strictly conserved resides are highlighted in red, and highly conserved resides are highlighted in yellow. Residues discussed in the main text are denoted by a star.

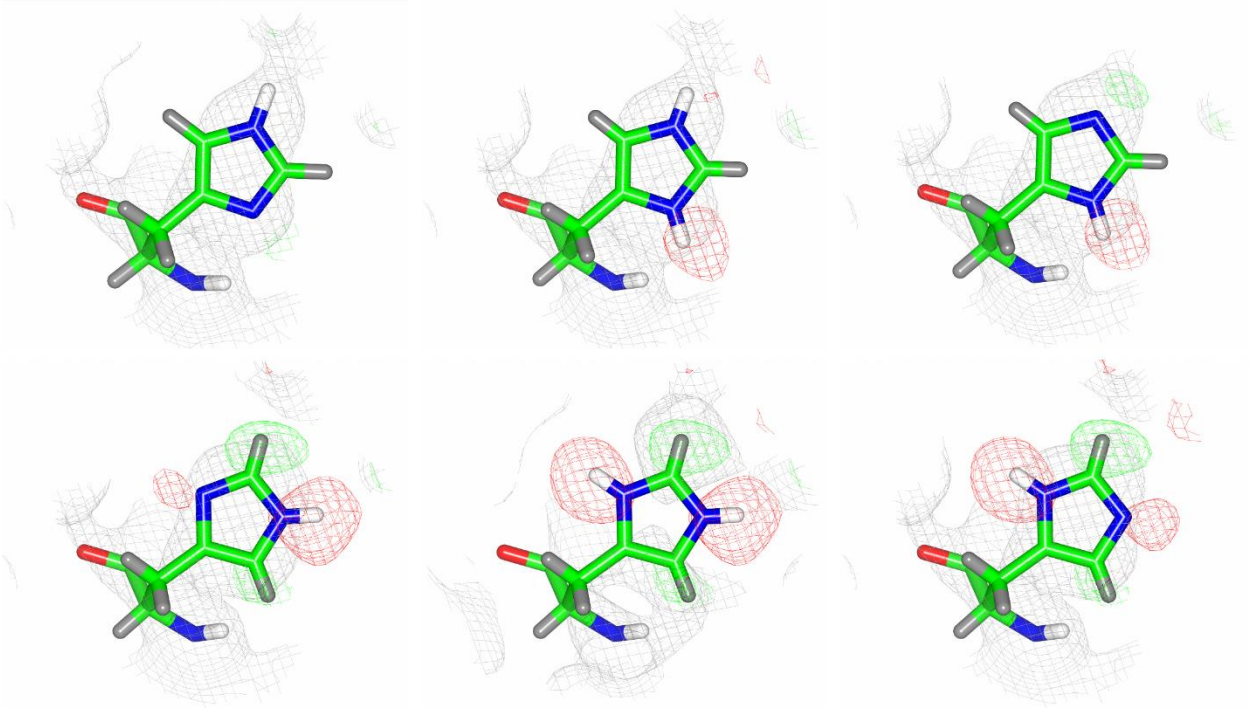

Figure S4. Fits of His157 conformational and protonation states with observed neutron scattering length density. Six forms of His157 were refined for both NCS molecules. (NCS molecule A is shown.) Neutron scattering length density (SLD) is shown in gray as $2F_O–F_C$ maps contoured at $\sigma = 1.0$. Positive and negative excess neutron SLD from $F_O–F_C$ maps contoured at $\sigma = 2.5$ is shown in green and red, respectively. The form shown at upper left was used in the joint X-ray/neutron refined model (PDB 5TKI).

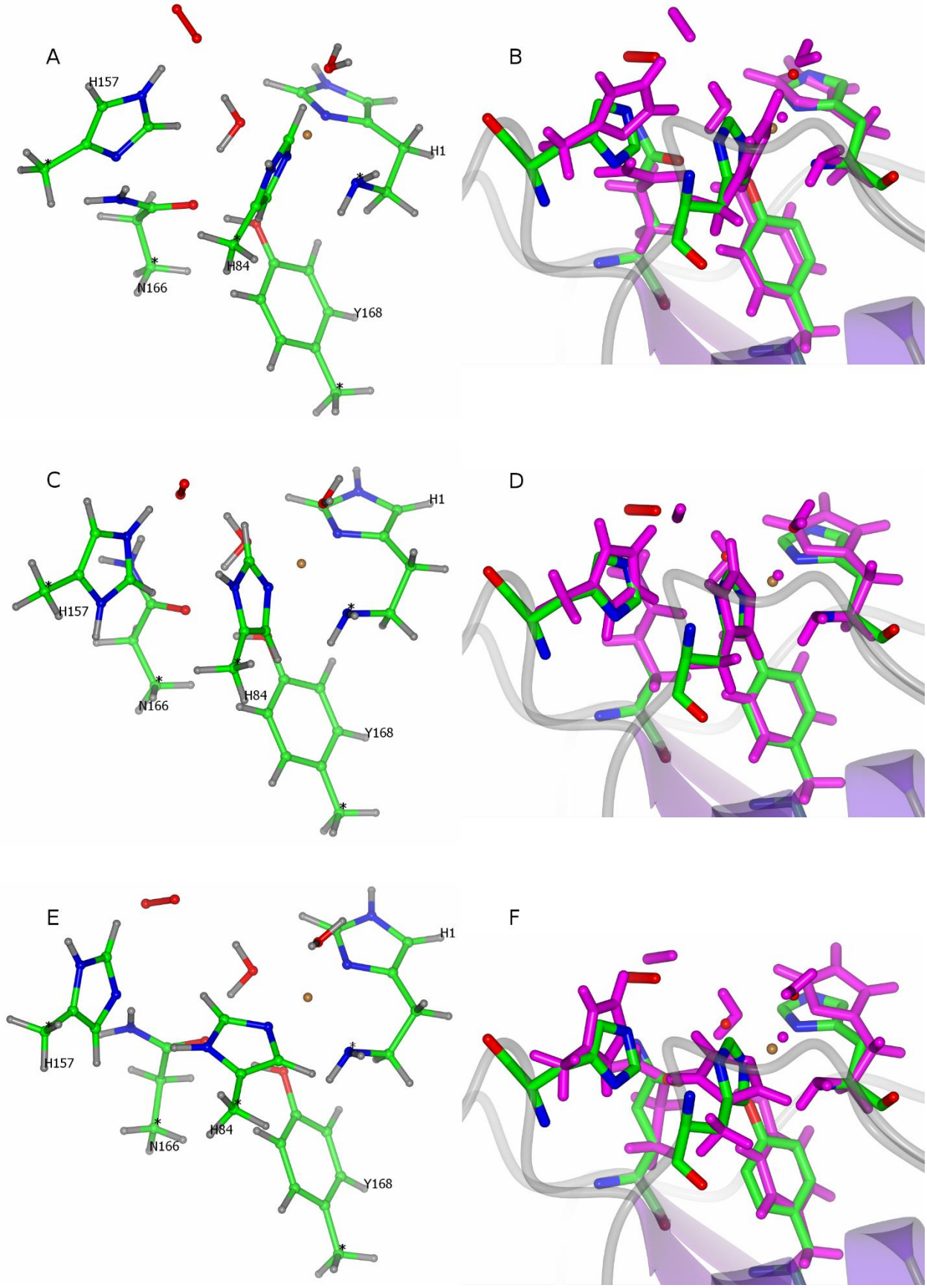
A
H157
H1
H84
N166
Y168
B
C
H1
H157
H84
N166
Y168
D
E
H1
H157
H84
N166
Y168
F

Figure S5. Geometry optimized DFT active site models and the same superimposed with NCS molecule B resting state active site structure (PDB 5TKG). For the superimposed structures, the active site models are colored in magenta. Panel A-B: “neutral” active site model. Panel C-D: “positive” active site model. Panel E-F: “neutral, flipped” active site model.

Table S5. Atomic coordinates of geometry optimized DFT active site models.

		neutral, flipped			positive			neutral		
residue	atom	X	y	z	x	y	z	x	y	z
His1	N	-2.38986	-0.69716	1.61173	2.36208	-0.66290	-1.61145	-2.11943	-1.43018	1.81345
His1	H2	-2.22257	0.29737	1.44727	2.27782	0.34053	-1.44547	-1.96529	-0.46293	2.10000
His1	H3	-2.27977	-0.82816	2.61709	2.05805	-0.80800	-2.57416	-1.92213	-1.97729	2.65354
His1	CA	-3.81072	-0.98818	1.28475	3.80215	-1.00963	-1.50661	-3.55431	-1.62007	1.46452
His1	HA	-4.00859	-0.59507	0.28575	4.21398	-0.46091	-0.65719	-3.84198	-0.83363	0.76428
His1	H	-4.46188	-0.46536	1.99203	4.32641	-0.67366	-2.40682	-4.16938	-1.51915	2.36381
His1	CB	-4.08216	-2.49356	1.33212	4.01672	-2.51396	-1.30652	-3.77215	-2.99529	0.82754
His1	HB1	-3.72929	-2.89832	2.29132	3.47942	-3.06967	-2.08677	-3.35911	-3.76815	1.49024
His1	HB2	-5.16135	-2.66392	1.30371	5.07836	-2.74003	-1.43774	-4.84467	-3.19220	0.75768
His1	CG	-3.44471	-3.20118	0.17938	3.58520	-2.94803	0.05801	-3.16917	-3.08655	-0.54002
His1	CD2	-3.98001	-4.10987	-0.69341	4.25372	-3.66832	1.01166	-3.71914	-3.55276	-1.70413
His1	HD2	-4.95741	-4.56154	-0.74456	5.22727	-4.13120	1.00871	-4.68740	-3.97668	-1.91604
His1	ND1	-2.13881	-2.93457	-0.21020	2.35653	-2.56729	0.57770	-1.88224	-2.63773	-0.81499
His1	CE1	-1.90023	-3.66386	-1.29676	2.28991	-3.04152	1.81748	-1.66877	-2.83335	-2.11529
His1	HE1	-0.98781	-3.66236	-1.86802	1.46758	-2.89628	2.49809	-0.77217	-2.56982	-2.65110
His1	NE2	-2.98747	-4.39018	-1.60869	3.41646	-3.71777	2.10753	-2.75610	-3.38772	-2.67666
His1	HE2	-3.06710	-5.01483	-2.39953	3.61672	-4.17136	2.98824	-2.84841	-3.63368	-3.65331
His84	CB	1.77894	1.76665	4.17943	-2.08016	1.50860	-4.01065	1.99450	1.90998	3.45482
His84	HB1	2.65120	1.42845	4.74869	-2.17045	1.07862	-5.01355	1.89623	1.93966	4.54458
His84	HB2	0.93541	1.84011	4.86808	-1.37139	2.33675	-4.06146	1.37040	2.70043	3.03490
His84	H	1.99629	2.7718	3.80289	-3.05906	1.91372	-3.73304	3.03677	2.13449	3.20546
His84	CG	1.44659	0.83251	3.07244	-1.60428	0.49344	-3.02474	1.57989	0.59298	2.90355
His84	CD1	0.31440	0.11216	2.80832	-0.47582	0.43184	-2.24994	0.65810	0.26545	1.94755
His84	HD1	-0.57654	0.07381	3.41260	0.31354	1.16464	-2.18655	0.03697	0.92911	1.36916
His84	ND2	2.30227	0.5369	2.02865	-2.29488	-0.66894	-2.72481	2.12533	-0.61626	3.29227
His84	HD2	3.23819	0.89985	1.88360	-3.17606	-0.95557	-3.12980	2.84194	-0.74276	3.99548
His84	CE1	1.68827	-0.31355	1.18593	-1.59095	-1.38075	-1.81711	1.54313	-1.61182	2.59121
His84	HE1	2.15850	-0.66865	0.28751	-1.91995	-2.31488	-1.38831	1.79590	-2.65335	2.71039
His84	NE2	0.46612	-0.59857	1.62508	-0.46958	-0.74115	-1.51006	0.64211	-1.10613	1.75764
His157	CB	7.23766	1.78495	1.45161	-7.35610	1.33663	-0.95981	6.83194	2.83725	-0.13862

		neutral, flipped			positive			neutral		
residue	atom	X	y	z	x	y	z	x	y	z
His157	HB1	7.42337	1.33241	2.43169	-7.17452	1.78390	-1.94256	6.46984	3.61058	0.54743
His157	HB2	6.87685	2.80284	1.61126	-7.69350	2.13196	-0.28721	6.75757	3.24154	-1.15394
His157	H	8.19699	1.84588	0.92676	-8.16761	0.61435	-1.06114	7.88701	2.65715	0.07794
His157	CG	6.23347	1.00781	0.66469	-6.14124	0.66140	-0.43717	6.04697	1.56566	0.00432
His157	CD2	5.02149	1.34887	0.10781	-5.90020	-0.63819	-0.08306	6.53810	0.33089	0.35384
His157	HD2	4.54106	2.31781	0.11791	-6.56063	-1.49035	-0.09558	7.53644	-0.00122	0.59149
His157	ND1	6.40773	-0.31769	0.31660	-4.94306	1.32558	-0.22011	4.67244	1.46690	-0.20434
His157	HD1	7.20562	-0.89158	0.55320	-4.78591	2.31427	-0.36610	--	--	--
His157	CE1	5.33417	-0.71623	-0.41525	-4.02459	0.46161	0.24383	4.36693	0.19974	0.01729
His157	HE1	5.23689	-1.71728	-0.80808	-3.00062	0.70410	0.49047	3.37851	-0.22881	-0.05858
His157	NE2	4.46618	0.26869	-0.56372	-4.59026	-0.73573	0.33615	5.45904	-0.52707	0.35905
His157	HE2	--	--	--	-4.03054	-1.66235	0.61698	5.48586	-1.51677	0.55535
Gln166	CB	0.55719	3.92806	-2.52961	-0.49949	3.72088	2.60619	-0.70692	3.95878	-2.84437
Gln166	HB1	0.08141	4.68934	-3.15259	-0.40952	4.66098	3.15588	-1.11576	4.36618	-3.77147
Gln166	HB2	1.56932	4.26870	-2.29229	-0.99570	3.93047	1.65507	-0.30438	4.79049	-2.25999
Gln166	H	-0.01214	3.85176	-1.60022	0.50916	3.36153	2.39625	-1.53182	3.51011	-2.29313
Gln166	CG	0.58291	2.58317	-3.28237	-1.29394	2.71322	3.44042	0.39092	2.93570	-3.18870
Gln166	HG1	-0.43585	2.25997	-3.51066	-0.76338	2.48616	4.37392	-0.05000	2.09089	-3.73072
Gln166	HG2	1.12080	2.69406	-4.22899	-2.26005	3.13424	3.74357	1.12232	3.39619	-3.85722
Gln166	CD	1.23078	1.50111	-2.44610	-1.55783	1.39155	2.73945	1.10331	2.35275	-1.98521
Gln166	NE2	2.54476	1.31728	-2.57603	-2.39700	0.53382	3.32784	2.39823	2.57987	-1.85632
Gln166	HE21	3.06406	1.88312	-3.23192	-2.82086	0.75002	4.21842	2.86918	3.13490	-2.55780
Gln166	HE22	3.09010	0.75144	-1.91163	-2.58400	-0.38039	2.90735	3.00585	2.21861	-1.10324
Gln166	OE1	0.54639	0.83307	-1.62363	-1.02533	1.10983	1.63330	0.47262	1.63972	-1.12817
Tyr168	CB	-5.08149	5.25240	0.81138	4.84070	5.27883	-1.10414	-5.79294	4.36090	1.47791
Tyr168	HB1	-5.08548	6.09622	0.11080	5.01011	6.04570	-0.33834	-6.07377	5.18337	0.80181
Tyr168	HB2	-4.64160	5.60806	1.74746	4.37047	5.77280	-1.95920	-5.41609	4.81884	2.39538
Tyr168	H	-6.12621	4.99070	1.00557	5.82479	4.91931	-1.42030	-6.70516	3.79847	1.68975
Tyr168	CG	-4.31159	4.07747	0.24848	3.98533	4.15755	-0.57267	-4.76240	3.51614	0.81433
Tyr168	CD1	-4.90569	3.20030	-0.67323	4.54755	3.11848	0.18353	-5.14610	2.41701	-0.01049
Tyr168	HD1	-5.94427	3.35074	-0.95710	5.62025	3.10602	0.35782	-6.20118	2.19467	-0.13080

		neutral, flipped			positive			neutral		
residue	atom	X	y	z	x	y	z	x	y	z
Tyr168	CD2	-2.97634	3.83872	0.59448	2.60182	4.13877	-0.78095	-3.37195	3.81219	0.96178
Tyr168	HD2	-2.48625	4.49036	1.31372	2.13912	4.92727	-1.36878	-3.07949	4.64973	1.58634
Tyr168	CE1	-4.19594	2.14911	-1.24769	3.76041	2.11124	0.73537	-4.20666	1.65463	-0.65143
Tyr168	HE1	-4.66207	1.49153	-1.97480	4.19820	1.32895	1.34760	-4.47924	0.82674	-1.29612
Tyr168	CE2	-2.24886	2.78174	0.03524	1.79659	3.13229	-0.24386	-2.41304	3.06736	0.32706
Tyr168	HE2	-1.21079	2.62162	0.31717	0.72241	3.14354	-0.40541	-1.35874	3.29745	0.43231
Tyr168	CZ	-2.85211	1.94073	-0.91008	2.37532	2.12170	0.53333	-2.81117	1.96196	-0.49968
Tyr168	OH	-2.19885	0.89636	-1.50544	1.63925	1.11552	1.10148	-1.96097	1.21769	-1.14208
Tyr168	HH	-1.22169	1.01003	-1.47009	0.69353	1.36447	1.18074	-0.92237	1.50019	-1.13513
Copper	CU	-0.87737	-1.71927	0.68548	0.98200	-1.53333	-0.38304	-0.62300	-1.91951	0.49636
Oxygen	O1	3.39169	-2.29823	-3.12227	-2.42843	-2.15822	1.92860	3.70441	-3.17427	-2.52793
Oxygen	O2	3.09489	-2.83528	-2.07394	-3.05499	-2.66702	0.86975	3.33494	-2.74898	-1.45269
Water1	O	0.28036	-1.71539	-1.04726	-0.07129	-1.43325	1.30540	0.56146	-1.19844	-1.09107
Water1	H	0.50046	-0.79102	-1.34916	-0.88134	-1.98661	1.51622	1.43170	-1.60305	-1.22428
Water1	H	1.06738	-2.26390	-1.16686	-0.41069	-0.51494	1.41487	0.69705	-0.22598	-1.09633
Water2	O	0.02505	-3.50609	1.67091	0.39729	-3.61060	-1.32105	0.18889	-3.98010	0.78455
Water2	H	0.57356	-3.43619	2.46425	0.06381	-3.87069	-2.19027	0.32901	-4.45523	1.61552
Water2	H	-0.43397	-4.35538	1.72701	0.82783	-4.39618	-0.95790	-0.17410	-4.63748	0.17362

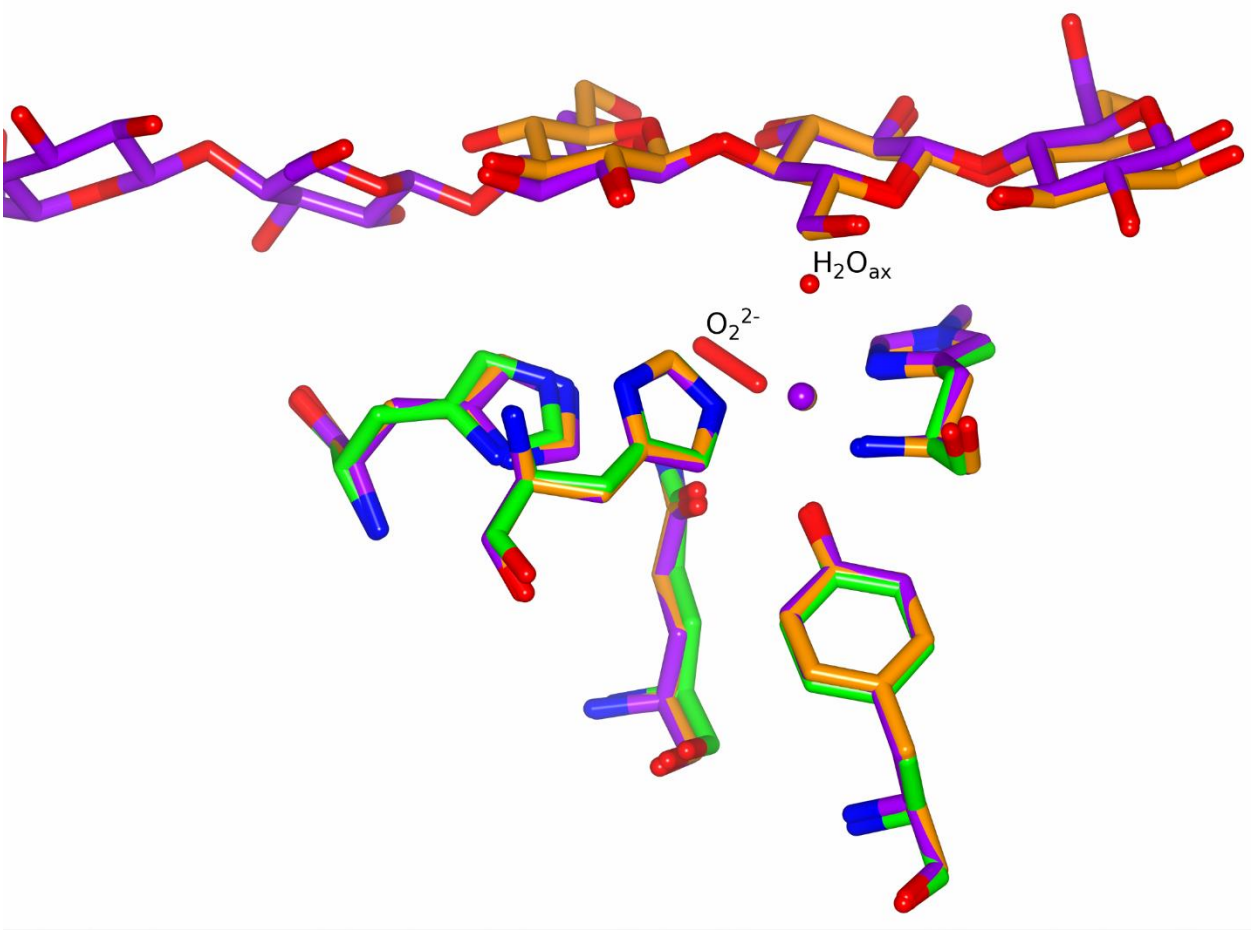

Figure S6. Superposition of copper–dioxo model (PDB 5TKH) with PDB 5ACJ and 5ACI. The active site of NCS molecule A from model 5TKH is shown in green with corresponding residues and substrates from 5ACJ and 5ACI shown in orange and purple, respectively. Non-hydrogen protein atoms were superimposed with RMSD = 0.25 Å (5THK–5ACJ) and RMSD = 0.29 Å (5TKH–5ACI).

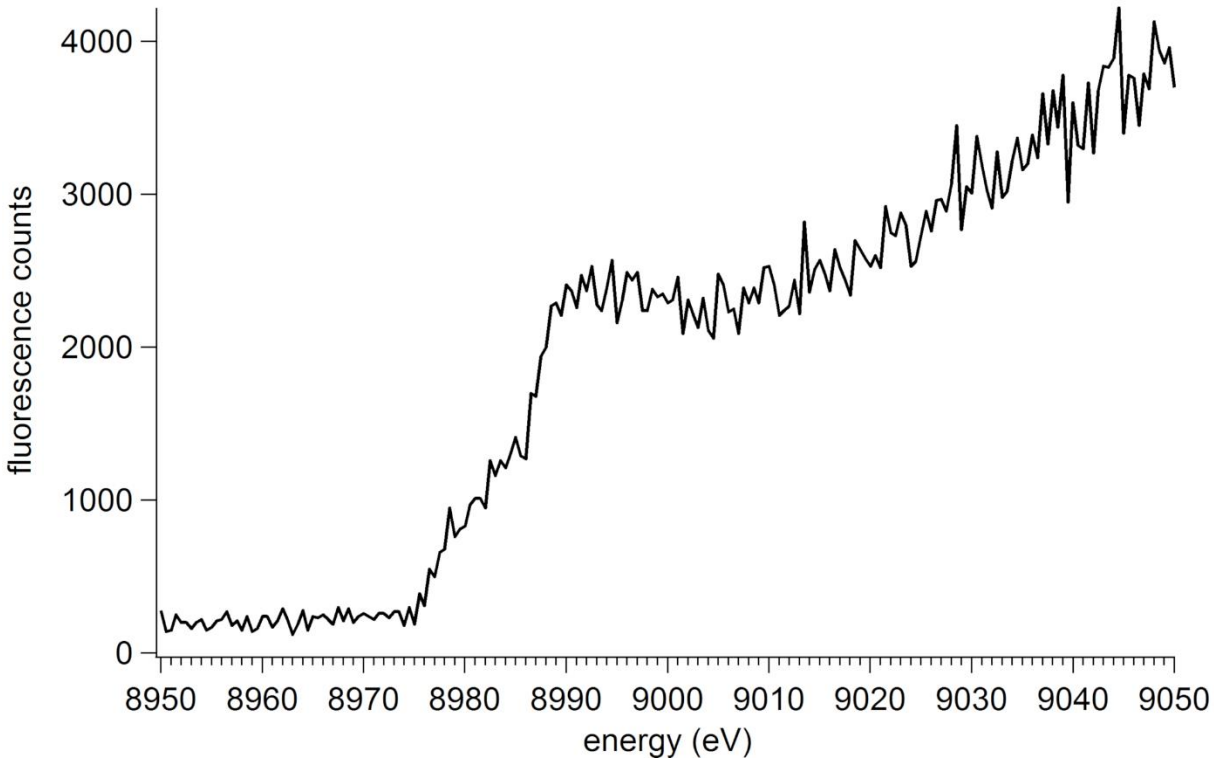

Figure S7. X-ray fluorescence scan of a *Nc*PMO-2 crystal near the copper K-edge. The center of the absorption edge is near 8984 eV which is indicative of a copper(I) species.